Chapter 3

# Separation and analysis of macroscopic currents

NICK B. STANDEN, NOEL W. DAVIES and PHILIP D. LANGTON

## 1. Introduction

In voltage clamp experiments, ionic flow is measured as electrical current. Macroscopic currents recorded from whole cells, or from relatively large areas of cell membrane, represent the sum of the ion fluxes through many channels, generally of more than one type. The first step in the interpretation of such currents is usually their separation into constituent components, each associated with a particular sort of ion channel. This chapter will consider some of the means by which this separation may be achieved, and will also give an introduction to methods for the analysis of the currents isolated in this way.

## 2. Current separation

In some experimental situations, the total membrane current may result almost entirely from ion flow through one type of channel, so that current separation is not necessary. This is often the case when currents flowing through transmitter-activated channels are elicited by the application of an agonist. When voltage clamp experiments involve a change in membrane potential, however, the situation is rarely so simple, since many types of channel are voltage-gated. In this case some means of current separation is needed. The initial process is often the removal of leakage and capacity currents by analogue compensation, by computer, or both, followed by methods of the type outlined below. Several of these methods involve the subtraction of currents recorded under one experimental condition from those under another, for example with and without a particular channel blocking substance. Such subtraction is usually done on the experimental current records themselves, but sometimes on their current-voltage relations. The widespread use of microcomputers together with programs for data acquisition and analysis has made this process straightforward. Subtraction does require, though, that currents should be relatively stable over the time period needed to change the experimental conditions, or at least that any change should be predictable enough to be controlled for.

Ion Channel Group, Department of Physiology, University of Leicester, PO Box 138, Leicester LE1 9HN, UK

Although the various strategies for current separation will be described separately, it is very common to combine two or more methods to isolate the current of interest; for example by using a blocking substance in combination with an appropriate voltage clamp protocol. Similar methods to those described below may also be applied to a novel cell type so as to characterize the channels present in terms of their permeant ionic species, pharmacology and voltage-dependence.

### Time of measurement

If the ionic channels that contribute to the total membrane current have sufficiently different kinetics, it may be possible to separate currents merely by measuring them at a suitable time during a voltage clamp pulse. For example, in squid axon, current measured at the end of a 10 ms depolarization will represent nearly pure current through delayed $K^+$ channels, as nearly all $Na^+$ channels will have inactivated by that time. Although this method may sometimes be adequate for the routine analysis of records, it needs experimental justification by one of the other methods described below.

### Ionic substitution

This method may be used to identify and separate currents in terms of the ionic species that carry charge. A classical example may be found in the study of squid
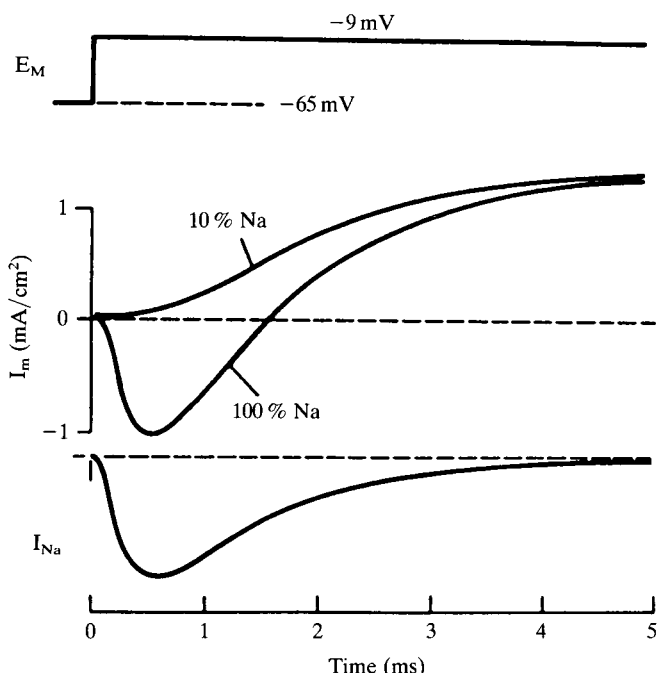


Fig. 1. Separation of $Na^+$ and $K^+$ currents in squid axon by ionic substitution. The low-sodium record (10% Na) is subtracted from that measured in sea water (100% Na) to give the $Na^+$ current shown below. (Reproduced with permission from Hille, 1984; after Hodgkin, 1958).

axon by Hodgkin & Huxley (1952a); see also Hodgkin (1958), shown in Fig. 1. Current was measured for a depolarization from $-65$ mV to $-9$ mV, first in sea water and then in artificial saline with only 10% of the $Na^+$ of sea water. In this preparation, where only two sorts of channel predominate, the current in 10% $Na^+$ is flowing through delayed rectifier $K^+$ channels, and the $Na^+$ channel current may be obtained by subtracting this current from the record in sea water (Fig. 1). If it is possible to perfuse the inside of the cell under study, ionic substitution may be applied to intracellular as well as extracellular solutions. Whole cell patch clamp is now the most common technique for recording macroscopic currents and, with this method, the composition of the pipette solution can normally be used to control the intracellular ionic composition, while a variety of perfusion methods for larger cells may be found in Kostyuk & Krishtal (1984).

Obviously ionic substitution alone cannot be used to separate currents through different channels which have the same major permeant ion, for example different types of $K^+$ channel. $Ca^{2+}$ channels also pose special problems, both because $Ca^{2+}$ entry may activate other channels (for example $K^+$ or $Cl^-$ channels) and because replacement of extracellular $Ca^{2+}$ by other ions can shift the voltage dependence of gating of many types of channel. So current records made in $Ca^{2+}$-free solution, or in the presence of $Ca^{2+}$ channel blockers, may not only lack $Ca^{2+}$ current, but also have altered currents through other channels. For this reason it is often necessary to use a combination of methods to separate currents through $Ca^{2+}$ channels. An example is illustrated in Fig. 3, and is discussed in the following section.

*Pharmacological separation*

Many substances are known that block ionic channels. These channel blockers form useful tools for the separation of currents, for the identification of channel types and also as ligands for use in the purification of channel proteins. Blockers range from simple inorganic ions through synthetic drugs to complex naturally occurring toxins. The range of blockers available is increasing as new toxins are discovered and new blocking compounds are synthesized, and so pharmacological methods provide increasingly powerful means of isolating currents through particular channel types. Blockers may act from the outside of the membrane, from the inside, or may be membrane permeant. Some block with high affinity, acting at nanomolar concentrations, while for others millimolar concentrations may be needed. Some blockers are specific for one type of channel, others may block several types, often with rather different affinities. An excellent account of blocking mechanisms is given by Hille (1992), and some blocking substances for different channels are given in Table 1 and the accompanying references.

Blocking substances are used in one of two main ways to separate currents. First, it may be possible to block all currents except the one that is of interest. Depending on the range of channels present, this may involve one or more blockers, sometimes in combination with ionic substitution. Secondly, a blocker specific for the channel of interest may be used. Current is recorded in the presence of the blocker and subtracted from that in its absence to yield the current required.

Table 1. *Some blockers for ion channels*

| Channel | Blocked by | References |
|---|---|---|
| Sodium | TTX, STX, local anaesthetics | Catterall (1980) |
| Calcium | | |
|   Generic calcium | $Co^{2+}$, $Cd^{2+}$, $Ni^{2+}$, $La^{3+}$ | Byerly & Hagiwara (1988) |
|   T-type | No specific ligand | |
|   L-type | Dihydropyridines: e.g. Nifedipine | Triggle & Janis (1987); |
| |   Phenylalkylamines: e.g. Verapamil |   Fox *et al.* (1987) |
| |   Benzothiazepines: e.g. Diltiazem | |
|   N-type | $\omega$-Conotoxin GVIA | Plummer *et al.* (1989) |
|   P-type | $\omega$-Agatoxin-IVA | Mintz *et al.* (1992) |
| Potassium | | |
|   Delayed rectifier | $TEA^+$, $Cs^+$, $Ba^{2+}$, Dendrotoxins, | Stanfield (1983); Cook & |
| |   4-Aminopyridine, Noxiustoxin, |   Quast (1990); Hille (1992) |
| |   Quinidine, Capsaicin, Phalloidin | |
|   A-current | $TEA^+$, 4-Aminopyridine, Quinidine, | Cook & Quast (1990); |
| |   Dendrotoxins |   Hille (1992) |
|   Inward rectifier | $Ba^{2+}$, $TEA^+$, $Cs^+$, $Rb^+$ | ” |
|   $Ca^{2+}$-activated | $TEA^+$, $Cs^+$, Quinidine, | ” |
| |   Charybdotoxin*, Apamin, | |
| |   Leiurotoxin I† | |
|   ATP-dependent | $Cs^+$, $Ba^{2+}$, sulphonylureas e.g. | Ashford (1990) |
| |   Glibenclamide | |
| Chloride | DIDS‡, IAA-94§, Furosemide, | Cabantchik & Greger (1992) |
| |   A9C‖, AABs¶, SITS** | |

*Selective for the large conductance $Ca^{2+}$-activated channel ($BK_{Ca}$)
†Selective for the small conductance $Ca^{2+}$-activated channel ($SK_{Ca}$)
‡DIDS: 4,4′-diisothiocyanatostilbene-2,2′-disulphonic acid
§IAA-94: indanyloxyacetic acid
‖A9C: anthracene-9-carboxylate
¶AABs: arylamino-benzoate derivates
**SITS: 4-acetamido-4′-isothiocyanatostilbene-2,2′-disulphonic acid

An example of a straightforward pharmacological separation of currents at the frog node of Ranvier is shown in Fig. 2. In this preparation, the $Na^+$ channel blocker tetrodotoxin (TTX) leaves only $K^+$ current flowing through delayed rectifier $K^+$ channels. Alternatively, the $Na^+$ current may be studied after block of the delayed $K^+$ channels with tetraethylammonium ions ($TEA^+$).

Fig. 3 shows an example of a more complex procedure in which a combination of methods is used to isolate the current flowing through $Ca^{2+}$ channels in a smooth muscle cell from a rat cerebral artery, recorded using whole cell patch clamp. To reduce $K^+$ currents as far as possible, $Cs^+$ is substituted for $K^+$ in the pipette solution that perfuses the cell interior. $Cs^+$ both acts as a $K^+$ substitute and as a $K^+$ channel blocker. The size of the $Ca^{2+}$ current is increased by raising external $[Ca^{2+}]$ to 10 mM. $Ca^{2+}$ current is obtained by subtraction using $Co^{2+}$ as a $Ca^{2+}$ channel blocker. Currents are first recorded in response to a series of voltage clamp pulses in an extracellular solution without $Co^{2+}$ (Fig. 3A). A rapid perfusion system is then used to apply solution to which 2 mM $Co^{2+}$ has been added and the voltage clamp series is
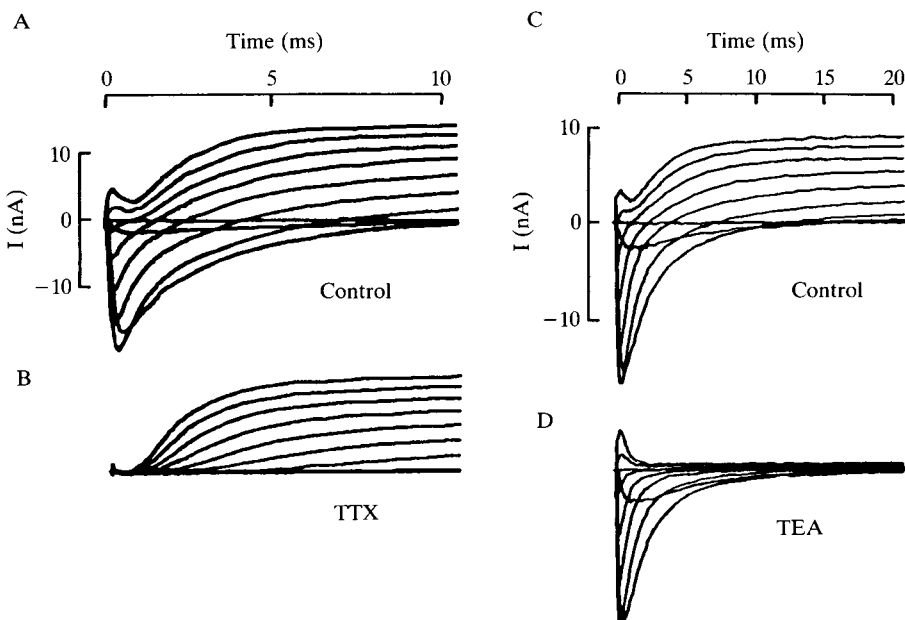
Fig. 2. Block of $Na^+$ and $K^+$ channels in frog node of Ranvier. (A) Control currents recorded when a node was depolarized to a series of potentials ranging from $-60$ mV to $+60$ mV in 15 mV steps. (The depolarization was preceded by a 40 ms hyperpolarization to $-120$ mV from the holding potential of $-90$ mV). (B) 300 nM TTX blocks $Na^+$ channels, leaving only $I_K$. (C) Control measurements in another node. (D) 6 mm TEA blocks $K^+$ channels, leaving $I_{Na}$. (Reproduced with permission from Hille, 1984).

repeated (Fig. 3B). The $Ca^{2+}$ currents (Fig. 3C) are obtained by subtracting the records in the presence of $Co^{2+}$ from those in its absence. Finally the stability of the currents with time may be checked by removing the $Co^{2+}$ again and recording a second set of currents in its absence.

*Voltage pulse protocol*

When the activation or inactivation of different channels occurs, at least in part, over different ranges of membrane potential, it may be possible to separate currents by choosing a suitable voltage pulse regime.

A good example of a current that may be isolated in this way is the early outward $K^+$ current, or A-current, first described in molluscan neurones, but which also occurs in vertebrate neurones and various other cell types. The channels carrying this current are usually almost fully inactivated at holding potentials close to the normal resting potential. Hyperpolarization removes the inactivation and the channels may then be opened by depolarization. The A-current may therefore be separated by subtraction of the current obtained in response to a depolarizing voltage step from the current recorded when the same step is applied preceded by a hyperpolarizing pulse, as shown in Fig. 4A.

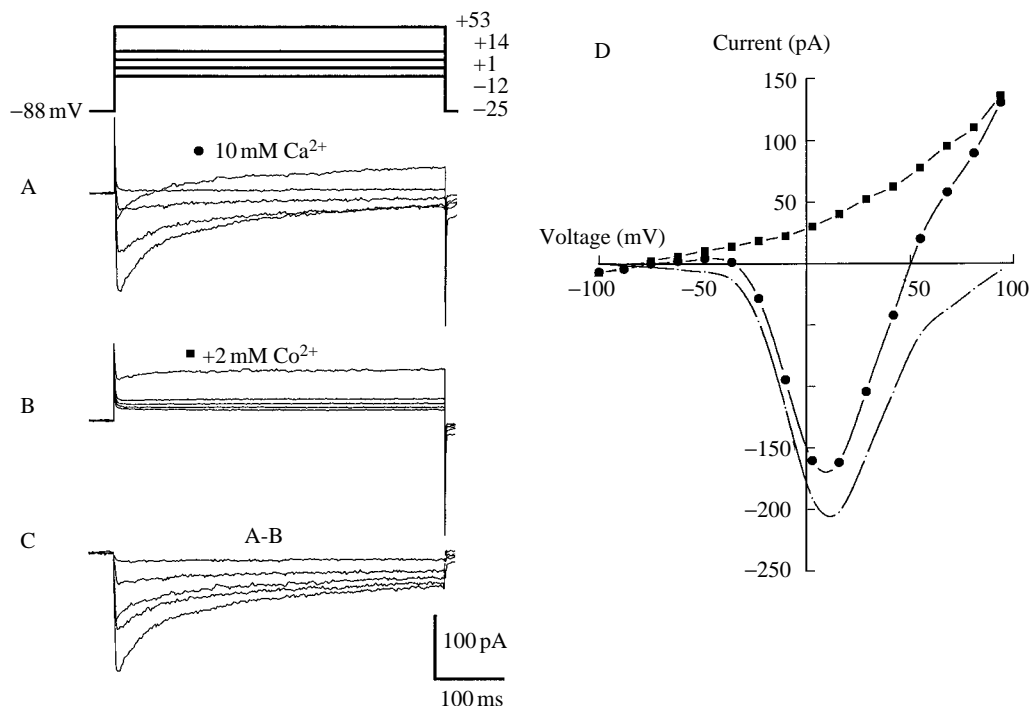Another method of separation that uses pulse protocol is the removal of all current

Fig. 3. Isolation of $Ca^{2+}$ channel current in an arterial smooth muscle cell. (A) Whole cell currents recorded in response to the depolarizing voltage steps shown above in external solution containing 10 mM $Ca^{2+}$. (B) Currents recorded during application of the 10 mM $Ca^{2+}$ solution to which 2 mM $CoCl_2$ was added to block currents through $Ca^{2+}$ channels. (C) $Ca^{2+}$ currents obtained by subtraction of records in B from those in A. (D) Corresponding current-voltage relations obtained in 10 mM $Ca^{2+}$ (●), 10 mM $Ca^{2+}$ + 2 mM $Co^{2+}$ (■), and for the current obtained by subtraction as A−B (broken line). The pipette (intracellular) solution contained (mM): CsCl, 130; $MgCl_2$, 1; EGTA 5, pH 7.2 with CsOH.

carried by a particular ion by making measurements at the equilibrium potential for that ion. For example, 'tails' of $Na^+$ or $Ca^{2+}$ current may be recorded when the membrane potential is returned to the $K^+$ equilibrium potential, $E_K$, after a depolarizing pulse. The method is illustrated for $Na^+$ current in Fig. 4B. A depolarizing pulse activates $Na^+$ channels so that an inward $Na^+$ current develops. The potential is then stepped to $E_K$ and the inward current jumps to a larger value as the driving force on $Na^+$ ions flowing through open $Na^+$ channels (= $V - E_{Na}$) is increased. The tail current then declines rapidly as $Na^+$ channels close at the hyperpolarized potential. The instantaneous value of the tail current measured immediately after the potential is changed to $E_K$ will be proportional to the number of $Na^+$ channels open at the end of the preceding pulse, and will be uncontaminated by $K^+$ current.

*Channel expression*

Virtually complete isolation of the ionic currents through a particular channel may be

possible by expressing the cloned channel in a cell type that contains little or no intrinsic ionic conductance. The most common method is to inject *Xenopus* oocytes with mRNA encoding a particular ion channel (see Dascal, 1987 for review). This mRNA is then translated by the oocyte and the channel protein becomes embedded in
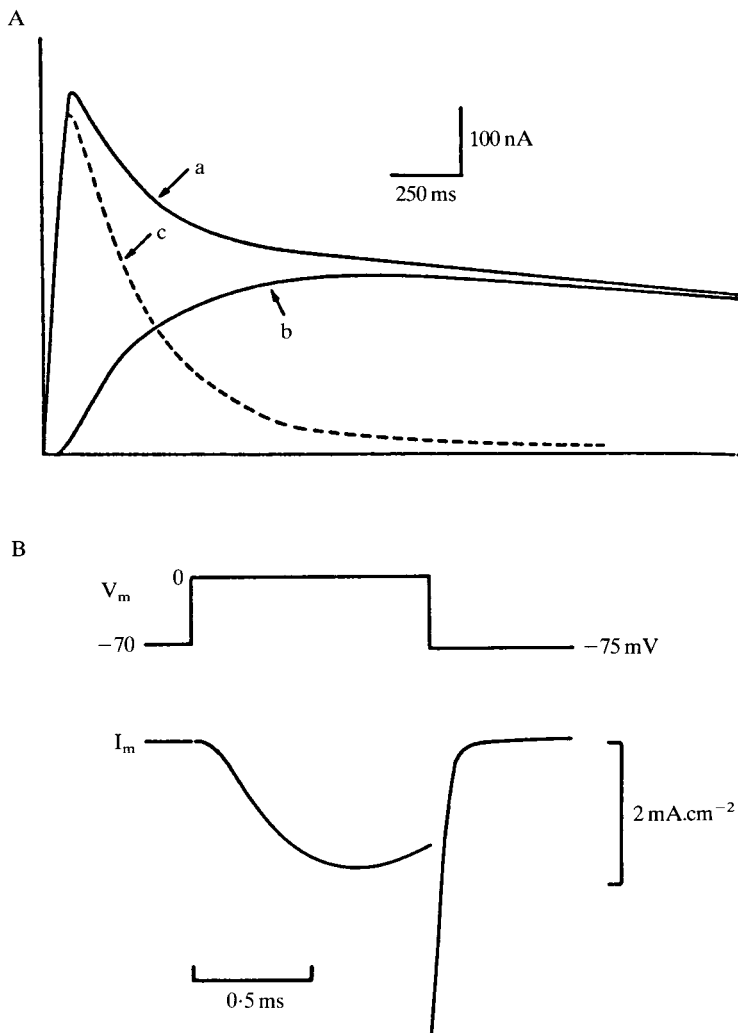


Fig. 4. (A) Separation of A-current in an *Anisodoris* neurone. Trace b shows current recorded for a step from −40 mV to −5 mV. This consists almost entirely of delayed $K^+$ current, $I_K$. If the holding potential is set to −80 mV, a step to −5 mV now activates both $I_K$ and A-current (trace a). Subtraction of b from a gives the A-current (broken line). For steps to potentials more negative than about −35 mV, $I_K$ is not activated, so that $I_A$ may be recorded directly. (Reproduced with permission from Connor & Stevens, 1971). (B) Sodium tail current in squid axon. The membrane potential is stepped to 0 mV for 1 ms so that $Na^+$ channels open, and is then repolarized to $E_K$ (−75 mV) when a rapidly declining tail of $Na^+$ current is seen. This figure and Fig. 7 have been drawn using a computer model of the voltage-clamped squid axon written by P. R. Stanfield and based on the equations given by Hodgkin & Huxley (1952b).

the membrane within 2 or 3 days. Although oocytes do have some intrinsic currents, the expressed currents are usually many times larger than this and can be studied in isolation. Other expression systems include some insect and mammalian cell lines that have almost no endogenous currents. An example is shown in Fig. 6, which shows currents recorded from a murine erythroleukaemia (MEL) cell transfected with DNA encoding a delayed rectifier current (hPCN1) from a human heart cDNA library (Shelton *et al*., 1993). MEL cells that have not been transfected do not have measurable voltage-activated currents, so that the currents measured represent pure currents through the expressed channel.

It is important to realise, however, that the current recorded from a cloned channel after expression may not always exactly reflect its behaviour in the native cell. This is because the subunit structure of the native and expressed channels may not always be the same, and because expressed channels may sometimes lack certain regulatory proteins even though they are still functional. This is particularly true of voltage-activated K^{+} channels which form as tetramers of individual subunits (Hille, 1992; Pongs, 1992). As such structural details become clearer, however, channel expression should provide an increasingly powerful method for studying the behaviour of a single type of channel in isolation.

## 3. Analysis of currents

There is only space here to give an outline of some of the basic methods available for the analysis of ionic currents recorded in macroscopic voltage clamp experiments. More detail and a wider variety of approaches may be found in the original literature. The book by Hille (1992) covers many techniques for the analysis of currents and also acts as a useful source of references to research papers.

*Current-voltage relations*

The first step in the analysis of an ionic current is often to summarize its voltage-dependence in the form of a current-voltage (*I-V*) relation. For transmitter-activated channels that show little voltage-dependent gating, the current-voltage relation can be obtained by measuring the current induced by application of the transmitter chemical at a series of different voltage-clamped potentials. The potential at which the current reverses direction (the reversal potential) gives information about which ion or ions may be carrying current through the transmitter-activated channel.

Examples of current-voltage relations for voltage-activated channels are shown in Fig. 5, which shows *I-V* relations for the peak Na^{+} current, $I_{Na}$, and delayed K^{+} current, $I_K$, of squid axon. $I_K$ first becomes measurable at about −50 mV and increases with further depolarization, both because more channels open and because the electrochemical driving force on K^{+} (the difference between the membrane potential, $V$, and the potassium equilibrium potential, $E_K$) increases. $I_{Na}$ first becomes increasingly negative (inward) as $V$ becomes more positive because depolarization leads to increasing numbers of open Na^{+} channels, but then starts to decrease again as
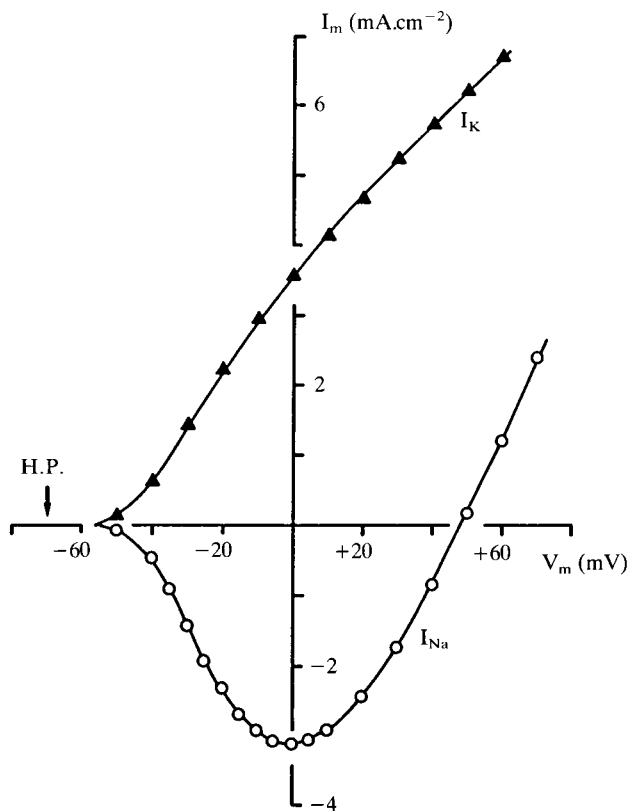
Fig. 5. Current-voltage relations for $I_{Na}$, and $I_K$ in squid axon. Peak $I_{Na}$ (○) and steady-state $I_K$ (▲) are plotted against the membrane potential during the voltage-clamp step. Holding potential −70 mV.

the reduction in driving force on Na$^+$ becomes more important. $I_{Na}$ becomes zero as the potential reaches $E_{Na}$, and at potentials positive to this the Na$^+$ current is outward. Thus the shape of the current-voltage relations for the current through these voltage-activated channels is determined both by the effect of membrane potential on channel open probability and by its effect on the driving force on the permeant ion.

*Activation curves and Boltzmann relations*

To describe the voltage-dependence of a voltage-activated channel we normally wish to study the way in which voltage affects channel gating independent of its effect on the electrochemical driving force. A way to extract the effect of voltage on channel gating alone is to measure instantaneous (or tail) currents at a fixed voltage, so that the driving force is constant. The method is very similar to that used to measure Na$^+$ current tails as described earlier, and an example taken from a cloned delayed rectifier K$^+$ channel, hPCN1, expressed in a cell line is shown in Fig. 6. Fig. 6A shows the voltage protocol used: a series of pulses in which the voltage is stepped from the

holding potential to a variable potential followed by return to a fixed voltage of −40 mV. The first depolarization leads to activation of $K^+$ channels, giving rise to the $K^+$ currents seen in Fig. 6B. On stepping to −40 mV the current jumps to an instantaneous value proportional to the number of channels open immediately before the voltage step, and then declines exponentially as channels close (Fig. 6C). Plotting the relative size of the instantaneous current against the voltage during the first depolarization gives a measure of the channel open probability as a function of voltage, usually called the activation curve (Fig. 6D).

The activation curve has a characteristic shape that reflects the nature of channel gating: the movement of charges in the voltage-sensitive region of the channel protein in the membrane voltage field. It may be fit by a Boltzmann relation of the form

$$\frac{I}{I_{max}} = \frac{1}{1 + \exp\left[(V_h - V)/k\right]} \tag{1}$$

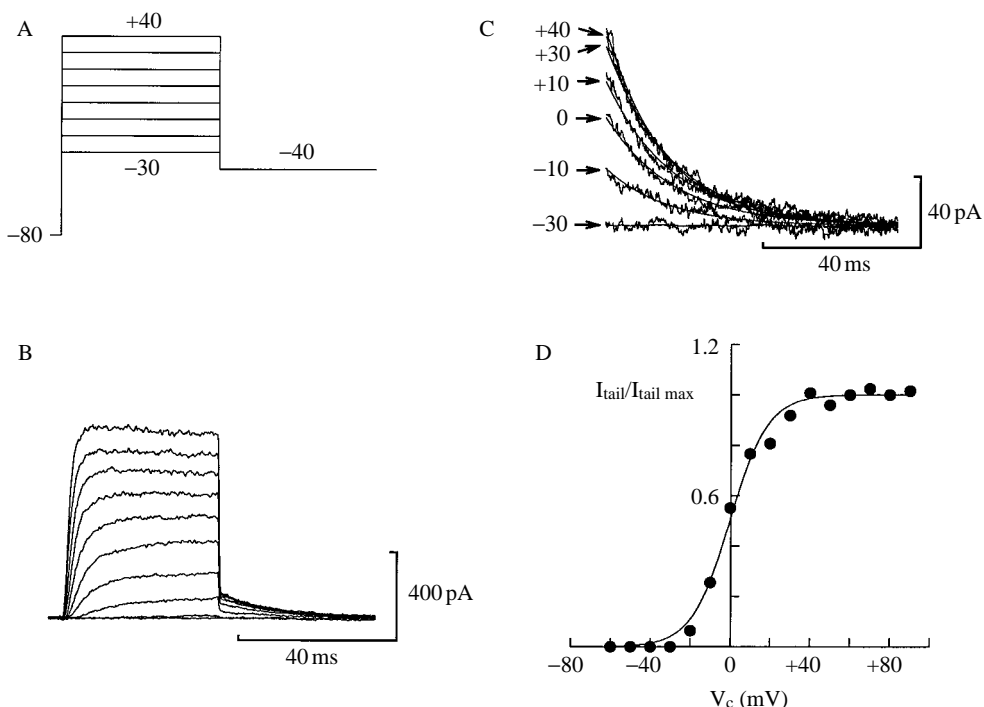where $I/I_{max}$ is the normalized instantaneous current, $V_h$ is the voltage at which half



Fig. 6. Measurement of the activation curve of a delayed rectifier $K^+$ channel using tail currents. The channel (hPCN1) was cloned from a human cDNA library and expressed in a murine erythroleukaemia cell. (A) The voltage-clamp protocol used. (B) The family of currents observed using whole cell patch clamp. Note the outward tail currents that occur after the membrane potential is returned to −40 mV. C shows these tail currents at a higher gain, together with exponential fits to their decline with time. (D) Activation relation obtained as described in the text. The curve is drawn according to the Boltzmann function of eqn (1) with $V_h = -0.1$ mV and $k = 9.3$ mV.

activation occurs, and $k$ is a factor determining how steeply the activation curve changes with voltage. The Boltzmann relation describes the voltage-dependence of channel gating, the factor $k$ showing the equivalent number of charges on the channel protein that move in the membrane voltage field to give rise to channel opening. One elementary charge will give $k = 24$ mV (channel open probability will change e-fold for a 24 mV change in voltage), while the $k$ of 9.3 mV for the curve of Fig. 6D corresponds to a gating charge of 2.6 elementary charges. Activation curves, and the parameters $V_h$ and $k$ of the Boltzmann fits to them, are used very commonly to characterize voltage-activated ion channels.

Single channel recording methods have provided measurements of the single channel current for many types of ion channel. This sometimes gives another way to construct an activation curve, which can be useful if for some reason it is difficult to measure tail currents, provided that the type of channel involved is known. The mean macroscopic current, $\bar{I}$, through a homogeneous population of ion channels will be given by $\bar{I} = Nip$, where $N$ is the total number of channels, $i$ is the single channel current, and $p$ the probability that a channel is open. The macroscopic current divided by the unitary current measured at the same voltage, $\bar{I}/i$, therefore equals $Np$, so that dividing the macroscopic $I$-$V$ relation by the single channel current-voltage relation gives the voltage-dependence of $Np$. If, as is usually the case, $N$ does not change over the course of the measurement, this is equivalent to the activation curve for the channel.

### Channel inactivation

Many ion channels, like $Na^+$ channels of squid axon, and many $Ca^{2+}$ and $K^+$ channels show inactivation as well as activation.

Inactivation can be studied using two-pulse experiments. The steady-state dependence of inactivation on membrane potential, also often called the inactivation curve or $h_\infty$ curve, can be measured with the pulse protocol shown in Fig. 7A. The first pulse (prepulse) is made long enough for inactivation to develop fully, and its voltage is varied, while the second (test) pulse of fixed size is used to measure the degree of inactivation. The current flowing during the test pulse is expressed relative to its size in the absence of a prepulse to generate the inactivation curve (Fig. 7B). In most cases channel inactivation is also voltage dependent, and can be fit by a Boltzmann function of the same type as that used to fit activation curves.

The time course of the development of inactivation at a particular potential can be measured using a prepulse of fixed voltage, but whose duration is varied. The membrane potential may be returned briefly to the holding level between the pre- and test pulses to allow channel activation to return to its resting level (e.g. Gillespie & Meves, 1980). Similarly, recovery from inactivation can be studied by varying the duration of the interval between a prepulse and a test pulse.

### Fitting the kinetics of currents

The kinetic analysis of current waveforms recorded under voltage-clamp is to some extent dependent on the type of model that is used to interpret channel gating. The
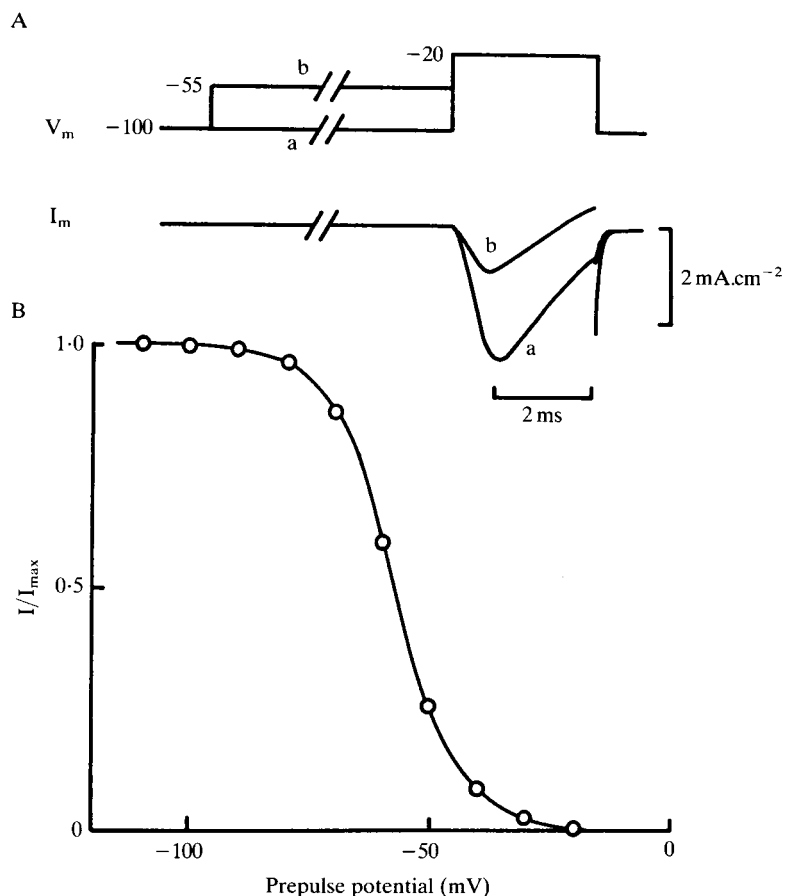
Fig. 7. (A) Measurement of steady-state $Na^+$ channel inactivation with a two-pulse experiment. The example traces show $I_{Na}$ for a depolarization to $-20$ mV with no prepulse and with a 50 ms prepulse to $-55$ mV. Holding potential $-100$ mV. (B) Steady-state $Na^+$ inactivation curve.

initial process in this analysis, however, is usually to fit a mathematical function to the experimental records of current, or to plots of conductance or of channel open probability against time. These may normally be fit by either an exponentially rising or falling function, or such a function raised to a power greater than one, or by the sum of such functions.

As an example, we may consider the time course of the increase in delayed potassium current in squid axon when the membrane potential is stepped from a value where the channels are shut to a level where they open significantly. The initial value of the current, $I_0$, will be zero if all channels are shut at the holding potential, and the rise of the current to its final value, $I_\infty$, may be fitted by

$$I_t = I_\infty (1 - e^{-t/\tau})^y \tag{2}$$

where $I_t$ is the current at time $t$ and $\tau$ is the time constant for activation. The power $y$ is 4 in this case, corresponding in the classical Hodgkin-Huxley formalism to the idea that four particles must move in the membrane to open a channel. A value of $y$ greater than one gives an initial delay in the rise of current, so that it follows a sigmoid time course.

If the membrane is repolarized to a potential where the channels will shut again, so that now $I_\infty = 0$, the current falls as

$$I_t = I_0(e^{-t/\tau})^y \tag{3}$$

where $I_0$ is the initial value of $I$ immediately after repolarization. This gives an exponential decline in current, with a time constant equal to $\tau/y$.

Many types of channel show both activation and inactivation, so that the current through them first increases and then declines with time. The necessary expression is then the product of a rising and a falling function. For example, assuming a holding potential where $I_0 = 0$, and that inactivation is exponential and will be complete at the step potential used

$$I_t = I'_\infty(1-e^{-t/\tau_1})^y . e^{-t/\tau_2} \tag{4}$$

$I'_\infty$ is now the maximum value which the current would reach in the absence of inactivation, and can be estimated from experimental records by measuring $\tau_2$, the time constant for inactivation, and multiplying the recorded $I_t$ by $e^{t/\tau_2}$ (e.g. Adams & Gage, 1979).

Having fit the macroscopic currents with exponential functions as described above, channel kinetics are usually described by some form of model. The models used most widely are still variants of that originally developed by Hodgkin & Huxley to analyse the currents recorded under voltage clamp from squid axon (Hodgkin & Huxley, 1952b; Hodgkin, 1958). The model describes channel gating in terms of the movement of charged particles in the cell membrane, and provides a powerful empirical description of channel kinetics. Hodgkin-Huxley descriptions have been developed for almost every type of voltage-dependent channel so far described, and the model is very clearly described by Hille (1992).

Equivalent models may be drawn in the form of state diagrams, which have become increasingly popular since the advent of single channel recording because they are also useful for interpreting kinetics at the single channel level. Such models envisage the channel as adopting several possible conformational states, each of which may correspond to the channel pore being either open or closed. The simplest model in which there is just one open and one closed state, with voltage dependent rate constants for transitions between them

$$C \rightleftharpoons O$$

will lead to an exponential change in channel open probability, and so current, in response to a step change in voltage. Sequential models, in which the channel passes through a series of closed states before opening, can predict a sigmoid rise in current.

An example originally proposed by Armstrong (1969) to describe delayed rectifier $K^+$ channel kinetics in squid axon is given below:

$$C4 \rightleftharpoons C3 \rightleftharpoons C2 \rightleftharpoons C1 \rightleftharpoons O$$

Here $C4$, $C3$, $C2$ and $C1$ are different closed states, while in state $O$ the channel is open. This type of model is further discussed in Chapter 7.

*Noise analysis of macroscopic currents gives information about single channels*

The macroscopic current recorded under voltage clamp is the sum of the current through many ionic channels. Even when the average number of channels open is constant, the exact number open will change from instant to instant. This variation will result in fluctuation of the measured current or 'noise'. The techniques of noise analysis exploit this fluctuation to obtain information about the underlying single channel events.

The single channel current, $i$, can be estimated by measuring the variance of the macroscopic current, $I$. If a series of measurements of $I$ are taken, $I_1$, $I_2$ .... $I_n$, the variance, $\sigma_I^2$ is given by (5)

$$\sigma_I^2 = \frac{1}{n} \sum_{j=0}^{n} (I_j - \bar{I})^2$$

and is usually calculated by computer. $\bar{I}$ is the mean current.

We assume that each individual channel that contributes to the macroscopic current passes a single-channel current which is either zero (when the channel is in a closed state) or $i$ (when the channel is open). Since the mean value of the macroscopic current will be given by $\bar{I} = Nip$ , where $N$ is the total number of channels and $p$ the channel open-state probability, it can be shown that the variance and the mean macroscopic current will be related by

$$\sigma_I^2 = \bar{I}i(1-p) \tag{6}$$

Equation 6 shows that the variance will be maximal when $p = 0.5$, so that half the channels are open on average, and will be zero when $p$ is either 0 or 1. Rearranging (6) gives

$$i = \frac{\sigma_I^2}{\bar{I}(1-p)} \tag{7}$$

so that if $p \ll 1$, the single-channel current $i$ may be measured by dividing the variance by the mean current. If the open-state probability is not so small, an alternative version of equation (7) may be used. Variance and mean current will also be related by

$$\sigma_I^2 = i\bar{I} - (\bar{I}^2/N) \tag{8}$$

which yields a parabolic relation between variance and mean current. (The variance is maximal when $p = 0.5$ and is zero when $p$ is 0 or 1). Experimental plots of variance

against mean may be fitted to equation (8) to give estimates for $i$, the single-channel current, and $N$, the total number of channels (e.g. Sigworth, 1980).

Experimentally the variance may be measured when the current is in a steady state, for example in the presence of a constant low concentration of acetylcholine to activate endplate channels (Anderson & Stevens, 1973). Alternatively, the time course of the variance throughout a voltage pulse can be measured by ensemble averaging the currents recorded from many repetitions of the same pulse, and subtracting the average from each individual record (Sigworth, 1980). Finally, noise analysis methods can also be used to give information about channel kinetics (see e.g. Neher & Stevens, 1977).

# References

ADAMS, D. J. & GAGE, P. W. (1979). Characteristics of sodium and calcium conductance changes produced by depolarization in an Aplysia neurone. *J. Physiol., Lond.* **289**, 143-161.

ASHFORD, M. L. J. (1990). Potassium channels and modulation of insulin secretion. In *Potassium Channels: Structure, Classification, Function and Therapeutic Potential*, (ed. N. Cook), pp. 181-231. Ellis Horwood.

ANDERSON, C. R. & STEVENS, C. F. (1973). Voltage-clamp analysis of acetylcholine produced end-plate current fluctuations at frog neuromuscular junction. *J. Physiol., Lond.* **235**, 655-691.

ARMSTRONG, C. M. (1969). Inactivation of the potassium conductance and related phenomena caused by quaternary ammonium ion injection in squid axons. *J. Gen. Physiol.* **54**, 553-575.

BYERLY, L. & HAGIWARA, S. (1988) Calcium channel diversity. In *Calcium and Ion Channel Modulation* (ed. A. D. Grinnell, D. Armstrong & M. B. Jackson), pp. 3-18. New York: Plenum.

CABANTCHIK, Z. I. & GREGER, R. (1992). Chemical probes for anion transporters of mammalian cell membranes. *Am. J. Physiol.* **262**, C803-C827.

CATTERALL, W. A. (1980). Neurotoxins that act on voltage-sensitive sodium channels in excitable membranes. *Ann. Rev. Pharmacol. Toxicol.* **20**, 15-43.

CONNOR, J. A. & STEVENS, C. F. (1971). Voltage clamp studies of a transient outward membrane current in gastropod neural somata. *J. Physiol., Lond.* **213**, 21-30.

COOK, N. S. & QUAST, U. (1990). Potassium channel pharmacology. In *Potassium Channels: Structure, Classification, Function and Therapeutic Potential*, (ed. N. Cook), pp. 181-231. Ellis Horwood.

DASCAL, N. (1987). The use of *Xenopus* oocytes for the study of ion channels. *CRC Crit. Rev. Biochem.* **18**, 317-387.

FOX, A. P., NOWYCKY, M. C. & TSIEN, R. W. (1987). Kinetic and pharmacological properties distinguishing three types of calcium currents in chick sensory neurones. *J. Physiol., Lond.* **394**, 149-172.

GILLESPIE, J. I. & MEVES, H. (1980). The time course of sodium inactivation in squid giant axons. *J. Physiol., Lond.* **299**, 289-307.

HILLE, B. (1984). *Ionic Channels of Excitable Membranes.* Sunderland: Sinauer.

HILLE, B. (1992). *Ionic Channels of Excitable Membranes.* 2nd Edition. Sunderland: Sinauer.

HODGKIN, A. L. (1958). Ionic movements and electrical activity in giant nerve fibres. *Proc. R. Soc. Lond. B* **148**, 1-37.

HODGKIN, A. L. & HUXLEY, A. F. (1952a). Currents carried by sodium and potassium ions through the membrane of the giant axon of *Loligo. J. Physiol., Lond.* **116**, 449-472.

HODGKIN, A. L. & HUXLEY, A. F. (1952b). A quantitiative description of membrane current and its application to conduction and excitation in nerve. *J. Physiol., Lond.* **117**, 500-544.

KOSTYUK, P. G. & KRISHTAL, O. A. (1984). Intracellular perfusion of excitable cells. (IBRO handbook series: Methods in the neurosciences; vol. 5). Chichester: Wiley.

MINTZ, M., VENEMA V. J., SWIDEREK, K. M., LEE, T. D., BEAN, B. P. & ADAMS, M. E. (1992). P-type calcium channels blocked by the spider toxin $\omega$-Aga-IVA. *Nature* **355**, 827-830.

NEHER, E. & STEVENS, C. F. (1977). Conductance fluctuations and ionic pores in membranes. *Ann. Rev. Biophys. Bioeng.* **6**, 345-381.

PLUMMER, M. R., LOGOTHESIS, D. E. & HESS, P. (1989). Elementary properties and pharmacological sensitivities of calcium channels in mammalian peripheral neurones. *Neuron* **2**, 1453-1463.

PONGS, O. (1992). Molecular biology of voltage-dependent potassium channels. *Physiol. Rev.* **72**, S69-S88.

SHELTON, P. A., DAVIES, N. W., ANTONIOU, M., GROSVELD, F., NEEDHAM, M., HOLLIS, M., BRAMMAR, W. J. & CONLEY, E. C. (1993). Regulated expression of $K^+$ channel genes in electrically silent mammalian cells by linkage to $\beta$-globin gene-activation elements. *Receptors and Channels* **1**, 25-37.

SIGWORTH, F. J. (1980). The variance of sodium current fluctuations at the node of Ranvier. *J. Physiol., Lond.* **307**, 97-129.

STANFIELD, P. R. (1983). Tetraethylammonium ions and the potassium permeability of excitable cells. *Rev. Physiol. Biochem. Pharmacol.* **97**, 1-67.

TRIGGLE, D. J. & JANIS, R. A. (1987). Calcium channel ligands. *Ann. Rev. Pharmacol. Toxicol.* **27**, 347-369.